

# Tighter upper bounds on the critical temperature of two-dimensional superconductors and superfluids: Approaching the supremum

Tingting Shi<sup>1,2</sup>, Wei Zhang<sup>1</sup>, and C. A. R. Sá de Melo<sup>2</sup>

<sup>1</sup> *Department of Physics, Renmin University of China, Beijing 100872, China and*

<sup>2</sup> *School of Physics, Georgia Institute of Technology, Atlanta, Georgia 30332, USA*

(Dated: March 11, 2022)

We discuss standard and tighter upper bounds on the critical temperature  $T_c$  of two-dimensional superconductors and superfluids versus particle density  $n$  or filling factor  $\nu$ , under the assumption that the transition from the normal to the superconducting (superfluid) phase is governed by the Berezinskii-Kosterlitz-Thouless (BKT) mechanism of vortex-antivortex binding and a direct relation between the superfluid density tensor and  $T_c$  exists. The standard critical temperature upper bound  $T_c^{up1}$  is obtained from the Glover-Ferrell-Tinkham sum rule for the optical conductivity, which constrains the superfluid density tensor components. However, we show that  $T_c^{up1}$  is only useful in the limit of low particle/carrier density, where it may be close to the critical temperature supremum  $T_c^{sup}$ . For intermediate and high particle/carrier densities,  $T_c^{up1}$  is far beyond  $T_c^{sup}$  for any given interaction strength. We demonstrate that it is imperative to consider at least the full effect of phase fluctuations of the order parameter for superconductivity (superfluidity) to establish tighter bounds over a wide range of densities. Using the renormalization group, we obtain the critical temperature supremum for phase fluctuations  $T_c^\theta$  and show that it is a much tighter upper bound to  $T_c^{sup}$  than  $T_c^{up1}$  for all particle/carrier densities. We conclude by indicating that if the  $T_c^\theta$  is exceeded in experiments involving single band systems, then a non-BKT mechanism must be invoked.

*Introduction:* Several recent experiments have studied the critical temperature  $T_c$  of two-dimensional (2D) superconductors as a function of carrier density  $n$  or filling factor  $\nu$  for various materials, including double- and triple-layered twisted graphene [1, 2], lithium-intercalated nitrides [3, 4] and sulphur-doped iron selenide [5]. In all these 2D systems, the authors [1–5] describe their results as evolving from the Bardeen-Cooper-Schrieffer to the Bose regime as  $n$  or  $\nu$  are changed from high to low, and have raised the issue of the existence of an upper bound on  $T_c$ . For one-band 2D systems with parabolic dispersion, the standard upper bound is known to be  $T_c^{up1} = \varepsilon_F/8$  [6, 7], in units where  $k_B = 1$ , with  $\varepsilon_F$  being the Fermi energy. Extensions of this result have been proposed to flat band and multiband systems [8]. However, the validity of such extensions has been questioned in recent work showing several counter examples where upper bounds are arbitrarily exceeded [9].

The question of the existence of an upper bound for  $T_c$  in superconductors and superfluids is of fundamental importance [10, 11]. Understanding the conditions under which such bounds exist for various systems is key to paving the way to designing materials where room temperature superconductivity can be achieved at ambient pressure, as suggested by measurements of the penetration depth of a variety of materials [12, 13]. However, upper bounds are practically useless if they are too far above the supremum (least upper bound) [14], thus when these upper bounds exist, it is essential to establish if they are tight, that is, if they are close to the supremum  $T_c^{sup}$ . Identifying tight upper bounds to  $T_c^{sup}$  is a much more difficult than merely determining a standard upper bound based on the kinetic energy [8], nevertheless this is precisely what we propose to describe next.

Here, we study two examples where tighter upper bounds on  $T_c$  can be established for one-band 2D systems: the continuum limit with parabolic dispersion, and the square lattice case with sinusoidal dispersion, both with spatially dependent but non-retarded interactions. We show that the standard upper bound obtained via the bare superfluid density  $\rho_s$  [6, 8], which is independent of interactions or symmetry of the order parameter, are practically useless away from the regime of ultralow carrier density  $n$  in the continuum or away from the limits of  $\nu \rightarrow 0$  or  $\nu \rightarrow 2$  in the square lattice, because they severely overestimate the supremum  $T_c^{sup}$ . To remedy this issue, we demonstrate that much tighter bounds can be obtained by investigating the renormalized superfluid density  $\rho_s^R$  rather than the bare superfluid density  $\rho_s$ , since  $\rho_s^R \leq \rho_s$  strictly holds. This relation arises physically because  $\rho_s$  is calculated in linear response theory, which does not include the existence of vortices and antivortices in the superconductor or superfluid. Large transverse current fluctuations, due to vortices and antivortices with quantized circulations, screen the bare  $\rho_s$  and renormalize it to  $\rho_s^R$ . Furthermore, we show that the phase fluctuation supremum  $T_c^\theta = \pi\rho_s^R/2$  as a function of  $n$  or  $\nu$  and establish that the supremum  $T_c^{sup}$  must be always lower or equal to  $T_c^\theta$ , that is  $T_c^{sup} \leq T_c^\theta$ . We also emphasize that tighter upper bounds for  $T_c$ , based on  $T_c^\theta$ , rely on the idea that the transition from the superconductor or superfluid to the normal state is driven by the Berezinskii-Kosterlitz-Thouless (BKT) [15, 16] vortex-antivortex unbinding mechanism. Finally, we conclude that if an experimental  $T_c$  exceeds the phase fluctuation supremum  $T_c^\theta$  then either the chosen model does not apply or a non-BKT mechanism for superconductivity and superfluidity must be invoked when the model applies.

*Continuum and Lattice Hamiltonians:* To construct tighter upper bounds on  $T_c$ , we discuss 2D continuum and lattice Hamiltonians. In the continuum, we start from the Hamiltonian density  $\mathcal{H}(\mathbf{r}) = \mathcal{H}_K(\mathbf{r}) + \mathcal{H}_I(\mathbf{r})$ , for a single band system in units where  $\hbar = k_B = 1$ . The kinetic energy density is  $\mathcal{H}_K(\mathbf{r}) = \sum_s \psi_s^\dagger(\mathbf{r}) \left[ -\frac{\nabla^2}{2m} \right] \psi_s(\mathbf{r})$ , and the interaction energy density is  $\mathcal{H}_I(\mathbf{r}) = \int d^2\mathbf{r}' V(\mathbf{r}, \mathbf{r}') \psi_\uparrow^\dagger(\mathbf{r}) \psi_\downarrow^\dagger(\mathbf{r}') \psi_\downarrow(\mathbf{r}') \psi_\uparrow(\mathbf{r})$ , with  $V(\mathbf{r}, \mathbf{r}') = -V_s g(|\mathbf{r} - \mathbf{r}'|/R)$ . The magnitude of the  $s$ -wave attractive interaction  $V_s$  has units of energy, and the dimensionless function  $g(|\mathbf{r} - \mathbf{r}'|/R)$  has spatial range  $R$ . Fermions with spin projection  $s$  at position  $\mathbf{r}$  are represented by the field operator  $\psi_s^\dagger(\mathbf{r})$ . In the square lattice, we start from an extended Fermi-Hubbard Hamiltonian  $H = -t \sum_{\langle ij \rangle, s} \psi_{is}^\dagger \psi_{js} + U \sum_{is} \hat{n}_{i\uparrow} \hat{n}_{i\downarrow} + \sum_{i < j, s, s'} V_{ij} \hat{n}_{is} \hat{n}_{js'}$ , where  $\hat{n}_{is} = \psi_{is}^\dagger \psi_{js}$  is the fermion number operator at site  $i$  with spin  $s$ . The nearest neighbor hopping is  $t$ , the local (on-site) interaction is  $U$ , and the interaction between fermions in sites  $i$  and  $j$  is  $V_{ij}$ .

*Hamiltonians in Momentum Space:* The Hamiltonians in momentum space, for both continuum and lattice, are

$$H = \sum_{\mathbf{k}s} \varepsilon_{\mathbf{k}} \psi_{\mathbf{k},s}^\dagger \psi_{\mathbf{k},s} + \sum_{\mathbf{k}\mathbf{k}'\mathbf{q}} V_{\mathbf{k}\mathbf{k}'} b_{\mathbf{k}\mathbf{q}}^\dagger b_{\mathbf{k}'\mathbf{q}}, \quad (1)$$

where  $b_{\mathbf{k}\mathbf{q}} = \psi_{-\mathbf{k}+\mathbf{q}/2, \downarrow} \psi_{\mathbf{k}+\mathbf{q}/2, \uparrow}$  is the pairing operator,  $\varepsilon_{\mathbf{k}} = \mathbf{k}^2/2m$  for the continuum, and  $\varepsilon_{\mathbf{k}} = -2t [\cos(k_x a) + \cos(k_y a)]$  for the square lattice. The summation over  $\mathbf{k}$  and  $\mathbf{k}'$  represent integrals in the continuum and discrete sums in the lattice. The momentum-space interaction  $V_{\mathbf{k}\mathbf{k}'}$  is the double Fourier transform of the real space interactions.

In the examples discussed below, we focus on  $s$ -wave pairing, and thus, we will use an expansion of the momentum space interaction  $V_{\mathbf{k}\mathbf{k}'}$  in terms of its continuum or lattice angular momentum [17–19] and keep only the  $s$ -wave component. In this case, the interaction potential can be approximated by the separable form

$$V_{\mathbf{k}\mathbf{k}'} = -V_s \Gamma_s(\mathbf{k}) \Gamma_s(\mathbf{k}'). \quad (2)$$

In the continuum, for an attractive well with depth  $V_s$  and radius  $R$ , the symmetry factor can be approximated by  $\Gamma_s(\mathbf{k}) = (1 + k/k_R)^{-1/2}$ , where  $k_R \sim R^{-1}$  plays the role of the interaction range in momentum space [20]. In the square lattice, which has  $C_4$  point group, the symmetry factor for conventional  $s$ -wave pairing is  $\Gamma_s(\mathbf{k}) = 1$ , when, for instance, only local attractive interactions are considered, while the symmetry factor for extended  $s$ -wave pairing is  $\Gamma_s(\mathbf{k}) = \cos(k_x a) + \cos(k_y a)$ , when, for example, nearest neighbor attractive interactions are included. For more general lattices,  $\Gamma_s(\mathbf{k})$  are given by the irreducible representations of the point group of the lattice [18] compatible with  $s$ -wave symmetry.

*Effective Action:* We introduce the chemical potential  $\mu$  and the order parameter for superfluidity  $\Delta$  in

terms of its modulus  $|\Delta|$  and phase  $\theta$ . The effective action is  $S_{\text{eff}} = S_{\text{sp}}(|\Delta|) + S_{\text{ph}}(|\Delta|, \theta)$ . The first contribution to  $S_{\text{eff}}$  is the saddle-point action  $S_{\text{sp}} = \sum_{\mathbf{k}} \left[ \frac{(\xi_{\mathbf{k}} - E_{\mathbf{k}})}{T} - 2 \ln(1 + e^{-E_{\mathbf{k}}/T}) \right] + \frac{|\Delta|^2}{TV_s}$ , where  $E_{\mathbf{k}} = \sqrt{\xi_{\mathbf{k}}^2 + |\Delta_{\mathbf{k}}|^2}$  is the energy of quasiparticles with  $\xi_{\mathbf{k}} = \varepsilon_{\mathbf{k}} - \mu$ , and  $\Delta_{\mathbf{k}} = \Delta \Gamma_s(\mathbf{k})$  is the order parameter function for  $s$ -wave pairing. The second contribution

$$S_{\text{ph}} = \frac{1}{2} \int dr \left\{ \sum_{ij} \rho_{ij} \partial_i \theta(r) \partial_j \theta(r) + \kappa_s [\partial_\tau \theta(r)]^2 \right\}, \quad (3)$$

represents the phase-only fluctuation action in the low frequency and long wavelength limit. Here, the integrals run over position and imaginary time  $r = (\mathbf{r}, \tau)$ , with  $\int dr \equiv \int_0^{1/T} d\tau \int d^2\mathbf{r}$ . In Eq. (3),

$$\rho_{ij} = \frac{1}{4L^2} \sum_{\mathbf{k}} [2n_{\text{sp}}(\mathbf{k}) \partial_i \partial_j \xi_{\mathbf{k}} - Y_{\mathbf{k}} \partial_i \xi_{\mathbf{k}} \partial_j \xi_{\mathbf{k}}], \quad (4)$$

is the superfluid density tensor, where  $\partial_i$  is the partial derivative with respect to momentum  $k_i$  with  $i = \{x, y\}$ . Here,  $n_{\text{sp}}(\mathbf{k}) = \frac{1}{2} [1 - (\xi_{\mathbf{k}}/E_{\mathbf{k}}) \tanh(E_{\mathbf{k}}/2T)]$  is the momentum distribution per spin state, and  $Y_{\mathbf{k}} = (2T)^{-1} \text{sech}^2(E_{\mathbf{k}}/2T)$  is the Yoshida function. The superfluid density tensor is diagonal  $\rho_{ij} = \rho_s \delta_{ij}$ , where  $\rho_s = (1/4mL^2) \sum_{\mathbf{k}} [2n_{\text{sp}}(\mathbf{k}) - (k_x^2/m) Y_{\mathbf{k}}]$  for the continuum and  $\rho_s = (ta^2/L^2) \sum_{\mathbf{k}} [\cos(k_x a) n_{\text{sp}}(\mathbf{k}) - t \sin^2(k_x a) Y_{\mathbf{k}}]$  for the square lattice. The second term in Eq. (3) is

$$\kappa_s = \frac{1}{4L^2} \sum_{\mathbf{k}} \left[ \frac{|\Delta_{\mathbf{k}}|^2}{E_{\mathbf{k}}^3} \tanh\left(\frac{E_{\mathbf{k}}}{2T}\right) + \frac{\xi_{\mathbf{k}}^2}{E_{\mathbf{k}}^2} Y_{\mathbf{k}} \right], \quad (5)$$

with  $\kappa_s = \kappa/4$ , where  $\kappa = \partial n / \partial \mu|_{T, V}$  is related to the thermodynamic compressibility  $\mathcal{K} = \kappa/n^2$ .

The phase of the order parameter can be separated as  $\theta(\mathbf{r}, \tau) = \theta_c(\mathbf{r}, \tau) + \theta_v(\mathbf{r})$ , where the  $\tau$ -dependent (quantum) term  $\theta_c(\mathbf{r}, \tau)$  is due to collective modes (longitudinal velocities), and the  $\tau$ -independent (classical) term  $\theta_v(\mathbf{r})$  is due to vortices (transverse velocities). This leads to the action  $S_{\text{ph}} = S_c + S_v$ , since the longitudinal and transverse velocities are orthogonal. The collective mode action is  $S_c = \frac{1}{2} \int dr \left[ \rho_s [\nabla \theta_c(r)]^2 + \kappa_s [\partial_\tau \theta_c(r)]^2 \right]$ , while the vortex action is  $S_v = \frac{1}{2T} \int d^2\mathbf{r} \rho_s [\nabla \theta_v(\mathbf{r})]^2$ . The vortex contribution arises from the transverse velocity  $\mathbf{v}_t = \nabla \theta_v(\mathbf{r})$ , where  $\nabla \cdot \mathbf{v}_t(\mathbf{r}) = 0$ , by using the relation  $\nabla \times \mathbf{v}_t(\mathbf{r}) = 2\pi \mathbf{z} n_v(\mathbf{r})$  where  $n_v(\mathbf{r}) = \sum_i n_i \delta(\mathbf{r} - \mathbf{r}_i)$ , is the vortex density and  $n_i = \pm 1$  is the vortex topological charge (vorticity) at  $\mathbf{r}_i$ . Using these relations, we write

$$S_v = 2\pi \frac{\rho_s}{2T} \sum_{i \neq j} n_i n_j G(\mathbf{r}_i - \mathbf{r}_j) + \sum_i \frac{E_c}{T} n_i^2, \quad (6)$$

where  $E_c$  is the vortex core energy, and  $G(\mathbf{r}_i - \mathbf{r}_j)$  is the interaction potential between the topological charges  $n_i$  and  $n_j$  satisfying Poisson's equation  $\nabla_{\mathbf{r}}^2 G(\mathbf{r} - \mathbf{r}') = 0$ .

*Critical Temperature:* The self-consistency relations for  $|\Delta|$  and  $\mu$  for a given temperature  $T$  are obtained from effective action  $S_{\text{eff}} = S_{\text{sp}} + S_{\text{ph}}$  as follows. The order parameter equation is obtained through the stationarity condition  $\delta S_{\text{sp}}/\delta \Delta^* = 0$ , leading to

$$\frac{1}{V_s} = \sum_{\mathbf{k}} \frac{|\Gamma_s(\mathbf{k})|^2}{2E_{\mathbf{k}}} \tanh\left(\frac{E_{\mathbf{k}}}{2T}\right). \quad (7)$$

To relate  $\mu$  and  $n = N/L^2$ , where  $N$  is the total number of particles per band and  $L^2$  is the area of the sample, we use the thermodynamic relation  $n = -\partial\tilde{\Omega}/\partial\mu|_{T,V}$ , with  $\tilde{\Omega} = \Omega/L^2$ , where  $\Omega$  is the thermodynamic potential [21]. This leads to the number equation  $n = n_{\text{sp}} + n_{\text{cm}} + n_{\text{zp}}$ . Here,  $n_j = -\partial\tilde{\Omega}_j/\partial\mu|_{T,V}$ , with  $j = \{\text{sp}, \text{cm}, \text{zp}\}$ . Here,  $n_{\text{sp}} = 2\sum_{\mathbf{k}} n_{\text{sp}}(\mathbf{k})$ , while  $n_{\text{cm}}$  and  $n_{\text{zp}}$  are obtained from their respective  $\tilde{\Omega}_j$  [21].

The critical temperature, within the BKT mechanism, is given by the Nelson-Kosterlitz [22] relation

$$T_c^\theta = \frac{\pi}{2} \rho_s^R(\mu, |\Delta|, T_c^\theta), \quad (8)$$

as  $T \rightarrow T_c^\theta$  from below, where

$$\rho_s^R = \rho_s - \frac{\rho_s^2}{2T} \lim_{\mathbf{q} \rightarrow 0} \frac{\langle n_v(\mathbf{q})n_v(-\mathbf{q}) \rangle}{|\mathbf{q}|^2}, \quad (9)$$

is the renormalized superfluid density. Here,  $n_v(\mathbf{q})$  is the Fourier transform of vortex density  $n_v(\mathbf{r})$ . From Eq. (9), it is clear that  $\rho_s^R \leq \rho_s$  at any temperature  $T$ , because the correlation function  $\mathcal{F} = \lim_{\mathbf{q} \rightarrow 0} \langle n_v(\mathbf{q})n_v(-\mathbf{q}) \rangle/|\mathbf{q}|^2$  is strictly non-negative, that is,  $\mathcal{F} \geq 0$ . This implies that the upper bound  $T_c^{\text{up1}}$  based on the bare superfluid density  $\rho_s$  [6, 8] is not tight, and therefore may severely overestimate the least upper bound, that is, the supremum  $T_c^{\text{sup}}$ . The relation in Eq. (8) must be viewed as the phase fluctuation supremum (least upper bound)  $T_c^\theta$  and as tighter upper bound to the supremum  $T_c^{\text{sup}}$ .

To establish  $T_c^\theta$ , we combine Eqs. (6) and (9) to obtain the solution of the renormalization group flow equations [23–25] leading to

$$y^2(l) - \frac{1}{2\pi^3} \left[ \frac{2}{K(l)} + \pi \ln K(l) \right] = A, \quad (10)$$

for running variables  $K(l)$  and  $y(l)$ . The initial conditions are  $K(0) = \rho_s/T$  and  $y(0) = \exp(-E_c/T)$ , satisfying the relation  $y(0) = \exp[-E_c K(0)/\rho_s]$ . The flow of  $\rho_s$  is described by  $K(\ell)$ , and the flow of the vortex fugacity is represented by  $y(\ell)$ . The constant  $A$  determines the family of flow curves in the  $K^{-1}$ - $y$  plane. In Fig. 1, the critical flow curve, for which  $A = [\ln \pi/2 - 1]/\pi^2 = -0.0278$ , is shown. The fixed point at  $(K_*^{-1}, y_*) = (\pi/2, 0)$  leads to the relation  $T_c^\theta/\rho_s^R = \pi/2$  in Eq. (8). From the intersection between the curve  $y(0) = \exp[-E_c K(0)/\rho_s]$  and the critical flow line, we obtain the relation  $T_c^\theta/\rho_s = K_c^{-1}$ ,

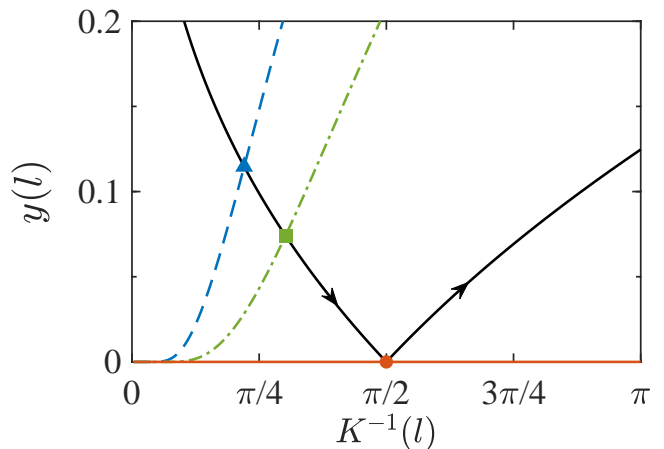


FIG. 1. Critical flow line (solid black) and examples of initial conditions  $y(0) = e^{-E_c K(0)/\rho_s}$  lines for  $E_c = 1.5\rho_s$  (dashed blue), for  $E_c = \pi^2\rho_s/4$  (dot-dashed green), and  $E_c \rightarrow \infty$  (solid red). The critical points are the solid blue triangle for  $E_c = 1.5\rho_s$ , the solid green square for  $E_c = \pi^2\rho_s/4$  (XY model), and the solid red circle for  $E_c \rightarrow \infty$ , which is also the fixed point of critical flow line. When  $E_c \rightarrow \infty$ ,  $T_c^\theta \rightarrow \pi\rho_s/2$ , thus for any  $E_c \leq \infty$ , then  $T_c^\theta = \rho_s/K_c \leq \pi\rho_s/2$ .

which allows to relate  $\rho_s^R$  and  $\rho_s$  via  $\rho_s^R = \rho_s(2/\pi K_c)$ . As seen in Fig. 1,  $K_c^{-1} \leq \pi/2$ , that is,  $(2/\pi K_c) \leq 1$  for any value of the vortex core energy  $E_c$ . Therefore,  $\rho_s^R$  is always less or equal to  $\rho_s$ , that is,  $\rho_s^R \leq \rho_s$ . The equality between  $\rho_s^R$  and  $\rho_s$  occurs only when  $E_c \rightarrow \infty$ .

An important consequence of  $\rho_s^R \leq \rho_s$  is that  $T_c^\theta = \pi\rho_s^R/2 \leq \pi\rho_s/2$ . Since the supremum  $T_c^{\text{sup}}$  is always upper-bounded by the phase fluctuation supremum  $T_c^\theta$ , that is,  $T_c^{\text{sup}} \leq T_c^\theta$ , it is clear that a lower upper bound is reached using  $\rho_s^R$  rather than  $\rho_s$ . Physically,  $T_c^\theta$  is a better upper bound to  $T_c^{\text{sup}}$  than  $T_c^{\text{ub0}} = \pi\rho_s(T=0)/2$  as suggested for superconductors with small superfluid density [11], where phase fluctuations are important. Furthermore,  $T_c^\theta$  is also a better upper bound of  $T_c^{\text{sup}}$  than  $T_c^{\text{ub1}} = \pi\rho_{s1}/2$ , where  $\rho_{s1} = (1/4L^2)\sum_{\mathbf{k}} 2n_{sp}(\mathbf{k})\partial_x^2 \xi_{\mathbf{k}}$  is the first term of Eq. (4) when  $\rho_{ij} = \rho_s\delta_{ij}$  and  $\xi_{\mathbf{k}}$  is isotropic in the continuum ( $C_\infty$  or  $SO(2)$  symmetric) or in the square lattice ( $C_4$  symmetric). In the continuum,  $\rho_{s1} \leq n/4m$  [6] is upper bounded, at any temperature  $T$ , by the ratio between the maximum pair density  $n/2$  and the fermion pair mass  $2m$  and reflects the Ferrell-Glover-Tinkham (FGT) [26–28] sum rule for the optical conductivity, first derived by Kubo [29]. This leads to the standard upper bound  $T_c^{\text{ub1}} = \varepsilon_F/8$  [6, 8], which is also known to apply to anisotropic superfluids [8, 30, 31], like those with spin-orbit coupling [30, 31]. For the square lattice,  $\rho_{s1} = (ta^2/L^2)\sum_{\mathbf{k}} \cos(k_x a)n_{sp}(\mathbf{k}) \leq t\nu/2$  [32], where  $\nu$  is the filling factor of the band, is also consistent with the FGT optical sum rule [33, 34]. Using particle-hole symmetry, a similar bound  $\rho_{s1} \leq t(2-\nu)/2$  applies, leading to the standard upper bound  $T_c^{\text{up1}} = t(\pi/4)\min\{\nu, (2-\nu)\}$ . The sequence of temperatures is

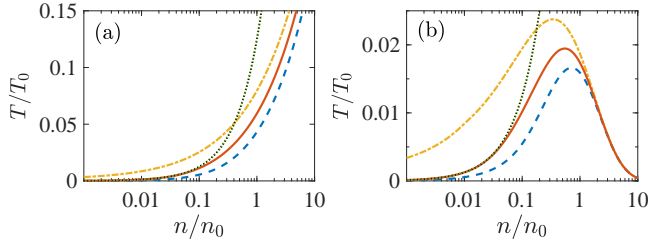


FIG. 2. Plots of  $T_c$  versus  $n$ , in units of  $\varepsilon_0 = k_0^2/2m = T_0$  and  $n_0 = k_0^2/2\pi$ . Results for zero-ranged interactions  $k_R \rightarrow \infty$  are shown in (a) and for finite-ranged interactions with  $k_R = k_0$  are shown in (b). In both panels the two-body binding energy is  $E_B = 0.01\varepsilon_0$ . The dotted black lines are  $T_c^{up1} = \varepsilon_F/8$ , the dotted green lines are  $T_c^{up0} = \pi\rho_s(T=0)/2$ , the dot-dashed yellow lines are  $T_c^{mf}$ , the solid red lines are  $T_c^\theta$  for  $E_c \rightarrow \infty$ , and the dashed blue lines are  $T_c^\theta$  for  $E_c = 1.5\rho_s$ .

$T_c^{sup} \leq T_c^\theta \leq T_c^{up0} \leq T_c^{up1}$ , with  $T_c^\theta$  being the best upper bound to  $T_c^{sup}$  and  $T_c^{up1}$  being the worst.

*Results:* The phase fluctuation supremum  $T_c^\theta$  is a much tighter upper bound to the supremum  $T_c^{sup}$  in comparison to both  $T_c^{up1}$  based on  $\rho_{s1}$ , and  $T_c^{up0}$  based on  $\rho_s(T=0)$ . This also applies to the saddle point (mean field) critical temperature  $T_c^{mf}$  obtained by neglecting phase fluctuations. The self-consistency relations determine  $\mu$ ,  $|\Delta|$  and  $T_c^\theta$  as functions of density  $n$  in the continuum or filling factor  $\nu$  in the square lattice for given interaction parameters.

In Fig. 2, we show  $T_c^\theta$ ,  $T_c^{up0}$ ,  $T_c^{up1}$ , and  $T_c^{mf}$  versus  $n$  for the cases of zero-ranged and finite ranged potentials. We use temperature/energy  $T_0 = \varepsilon_0 = k_0^2/2m$  and density  $n_0 = k_0^2/2\pi$  units, where  $k_0$  is a reference momentum related to the unit cell length  $a$  of a crystal ( $k_0 = 2\pi/a$ ) or to the laser wavelength  $\lambda$  in a cold atom system ( $k_0 = 2\pi/\lambda$ ), in which case,  $k_0$  ( $\varepsilon_0$ ) represents the recoil momentum (energy). We convert the interaction  $V_s$  with range  $k_R$  into the two-body binding energy  $E_B$  [35] to compare more easily the cases of zero and finite ranges. In comparison to the phase fluctuation supremum  $T_c^\theta$  (solid red line) for  $E_c \rightarrow \infty$ , the standard upper bound  $T_c^{up1}$  (dotted black line) fails miserably at intermediate and high densities  $n$  being practically useless in that regime. For parabolic bands,  $T_c^{up0}$  (dotted green line) is equal to  $T_c^{up1}$  for all  $n$  due to Galilean invariance. Furthermore,  $T_c^{mf}$  is always larger than  $T_c^\theta$ , exceeds  $T_c^{up1} = T_c^{up0}$  at lower densities, and is only reliable at larger densities.

In Fig. 3, we show  $T_c^\theta$ ,  $T_c^{up0}$ ,  $T_c^{up1}$ , and  $T_c^{mf}$  versus  $\nu$  for  $V_s/t = 3$ . In panel (a)  $\Gamma_s(\mathbf{k}) = 1$  (conventional s-wave) and in (b)  $\Gamma_s(\mathbf{k}) = \cos(k_x a) + \cos(k_y a)$  (extended s-wave) [36]. In comparison to the phase fluctuation supremum  $T_c^\theta$  (solid red line) for  $E_c \rightarrow \infty$ , the standard upper bound  $T_c^{up1}$  (dotted black line) fails miserably at intermediate fillings  $\nu$ , where even  $T_c^{mf}$  is a better upper bound, however  $T_c^{up1}$  is tighter for  $\nu \sim 0$  or  $\nu \sim 2$ . Notice that  $T_c^{up0}$  is always a better upper bound than

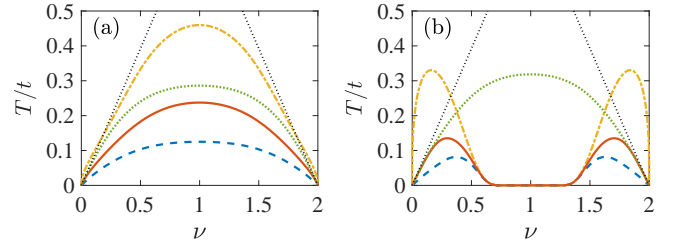


FIG. 3. Plots of  $T_c$  versus  $\nu$ . In both panels the interaction parameter is  $V_s/t = 3$ . In (a)  $\Gamma_s(\mathbf{k}) = 1$  (conventional s-wave), and in (b)  $\Gamma_s(\mathbf{k}) = \cos(k_x a) + \cos(k_y a)$  (extended s-wave). The dotted black lines are the standard upper bound  $T_c^{up1} = t(\pi/4)\min\{\nu, (2-\nu)\}$ , the dotted green lines are  $T_c^{up0} = \pi\rho_s(T=0)/2$ , the dot-dashed yellow lines are  $T_c^{mf}$ , the solid red lines are  $T_c^\theta$  for  $E_c \rightarrow \infty$ , and the dashed blue lines are  $T_c^\theta$  for  $E_c = 1.5\rho_s$ .

$T_c^{up1}$ , and while in (a) it is not too far above  $T_c^\theta$ , in (b) it overestimates substantially  $T_c^\theta$  at intermediate  $\nu$ , where the order parameter modulus  $|\Delta|$  vanishes. In (a),  $T_c^{mf}$  is always above all upper bounds for  $\nu \sim 0$  and  $\nu \sim 2$ , but below  $T_c^{up1}$  and above  $T_c^{up0}$  and  $T_c^\theta$  at intermediate  $\nu$ . While in (b),  $T_c^{mf}$  is above all upper bounds for  $\nu \sim 0$  or  $\nu \sim 2$ , but at intermediate values of  $\nu$  it is below  $T_c^{up1}$  and  $T_c^{up0}$ , but always above  $T_c^\theta$ . Quantum Monte Carlo (QMC) data [37] on  $T_c$  versus  $\nu$  for the attractive Hubbard model in (a) are bounded by  $T_c^\theta$ .

*Beyond Phase Fluctuations:* We remark that effects beyond phase fluctuations (longitudinal and transverse), such as modulus fluctuations of the order parameter, are not included in the phase fluctuation action describing the BKT mechanism for 2D superconductivity/superfluidity. Modulus fluctuations may further renormalize the superfluid density  $\rho_s$  and the compressibility  $\kappa_s$  [38], however these effects can only reduce  $T_c^\theta$ . Thus, we can safely regard  $T_c^\theta$  as the phase fluctuation supremum critical temperature for any given  $E_c$ .

*Conclusions:* We investigated tighter upper bounds on the critical temperature of two-dimensional (2D) superconductors and superfluids with a single parabolic (cosinusoidal) band in the continuum (square lattice). Using the renormalization group, we obtained the phase fluctuation supremum critical temperature  $T_c^\theta$  as the best upper bound for the supremum  $T_c^{sup}$  within the Berezinskii-Kosterlitz-Thouless (BKT) vortex-antivortex binding mechanism. We showed that standard upper bounds which are independent of interactions and order parameter symmetry are only useful at extremely low carrier density and practically useless anywhere else. Our results have important implications on measurements of  $T_c$  for one band superconductors/superfluids with non-retarded interactions, showing that any measurements that exceed  $T_c^\theta$  must arise from a non-BKT mechanism.

We thank the National Key R&D Program of China (Grant 2018YFA0306501), the National Natural Science Foundation of China (Grants 11522436 & 11774425), the

Beijing Natural Science Foundation (Grant Z180013), and the Research Funds of Renmin University of China (Grants 16XNLQ03 & 18XNLQ15) for financial support.

- 
- [1] Y. Cao, V. Fatemi, S. Fang, K. Watanabe, T. Taniguchi, E. Kaxiras, and P. Jarillo-Herrero, Unconventional superconductivity in magic-angle graphene superlattices, *Nature* **556**, 43 (2018).
- [2] J. M. Park, Y. Cao, K. Watanabe, T. Taniguchi, P. Jarillo-Herrero, Tunable strongly coupled superconductivity in magic-angle twisted trilayer graphene, *Nature* **590**, 249 (2021).
- [3] Y. Nakagawa, Y. Saito, T. Nojima, K. Inumaru, S. Yamanaka, Y. Kasahara, and Y. Iwasa, Gate-controlled low carrier density superconductors: Toward the two-dimensional BCS-BEC crossover, *Phys. Rev. B* **98**, 064512 (2018).
- [4] Yuji Nakagawa, Yuichi Kasahara, Takuya Nomoto, Ryotaro Arita, Tsutomu Nojima, Yoshihiro Iwasa, Gate-controlled BCS-BEC crossover in a two-dimensional superconductor, *Science* **372**, 190 (2021).
- [5] Y. Mizukami, M. Haze, O. Tanaka, K. Matsuura, D. Sano, J. Böker, I. Eremin, S. Kasahara, Y. Matsuda, and T. Shibauchi, Thermodynamics of transition to BCS-BEC crossover superconductivity in  $\text{FeSe}_{1-x}\text{S}_x$ , arXiv:2105.00739v1 (2021).
- [6] S. S. Botelho and C. A. R. Sá de Melo, Vortex-Antivortex Lattice in Ultracold Fermionic Gases, *Phys. Rev. Lett.* **96**, 040404 (2006).
- [7] A similar expression relating  $T_c$  to  $\epsilon_F$  at small densities was obtained by V. P. Gusynin, V. M. Loktev and S. G. Sharapov, Pseudogap phase formation in the crossover from Bose-Einstein condensation to BCS superconductivity, *JETP* **88**, 685 (1999). However, these authors did not recognize that this relation corresponds to an upper bound to  $T_c$  for all densities, independent of interaction strength.
- [8] T. Hazra, N. Verma, and M. Randeria, Bounds on the Superconducting Transition Temperature: Applications to Twisted Bilayer Graphene and Cold Atoms, *Physical Review X* **9**, 031049 (2019).
- [9] J. S. Hofmann, D. Chowdhury, S. A. Kivelson, and E. Berg, Heuristic bounds on superconductivity and how to exceed them, arXiv:2105.09322v2 (2021).
- [10] I. Esterlis, S. Kivelson, and D. Scalapino, A bound on the superconducting transition temperature, *npj Quantum Materials* **3**, 1 (2018).
- [11] V. J. Emery and S. A. Kivelson, Importance of phase fluctuations in superconductors with small superfluid density, *Nature* **374**, 434 (1995).
- [12] Y. J. Uemura, G. M. Luke, B. J. Sternlieb, J. H. Brewer, J. F. Carolan, W. N. Hardy, R. Kadono, J. R. Kempton, R. F. Kiefl, S. R. Kretzmann, P. Mulhern, T. M. Rise-man, D. L. Williams, B. X. Yang, S. Uchida, H. Takagi, J. Gopalakrishnan, A. W. Sleight, M. A. Subramanian, C. L. Chien, M. Z. Cieplak, Gang Xiao, V. Y. Lee, B. W. Statt, C. E. Stronach, W. J. Kossler, and X. H. Yu, Universal Correlations between  $T_c$  and  $n_s/m^*$  (carrier density over effective mass) in high- $T_c$  cuprate superconductors, *Phys. Rev. Lett.* **62**, 2317 (1989).
- [13] Y. J. Uemura, L. P. Le, G. M. Luke, B. J. Sternlieb, W. D. Wu, J. H. Brewer, T. M. Rise-man, C. L. Seaman, M. B. Maple, M. Ishikawa, D. G. Hinks, J. D. Jorgensen, G. Saito, and H. Yamochi, Basic similarities among cuprate, bismuthate, organic, Chevrel-phase, and heavy-fermion superconductors shown by penetration-depth measurements, *Phys. Rev. Lett.* **66**, 2665 (1991).
- [14] To illustrate the point with an analogy, consider the distance between the Earth and the Moon, which is certainly smaller than the distance between the Earth and the Sun. However, using the Earth-Sun distance as an upper bound for the Earth-Moon distance is certainly an overkill, as the Moon apogee is the least upper bound (supremum) for the Earth-Moon distance.
- [15] V. L. Berezinskii, Destruction of long-range order in one-dimensional and two-dimensional systems having a continuous symmetry group : I. Classical systems, *Sov. Phys. JETP* **32**, 493 (1970).
- [16] J. M. Kosterlitz and D. Thouless, Long-range order and metastability in two dimensional solids and superfluids: Application of dislocation theory. *J. Phys. C* **5**, L124 (1972).
- [17] R. D. Duncan and C. A. R. Sá de Melo, Thermodynamic properties in the evolution from BCS to Bose-Einstein condensation for a d-wave superconductor at low temperatures, *Phys. Rev. B* **62**, 9675 (2000).
- [18] J. F. Annett, Symmetry of the order parameter for high-temperature superconductivity, *Advances in Physics* **39**, 83 (1990).
- [19] M. Iskin and C. A. R. Sá de Melo, Superfluidity of p-wave and s-wave atomic Fermi gases in optical lattices *Phys. Rev. B* **72**, 224513 (2005).
- [20] This parametrization is necessary to produce a separable potential in momentum space that behaves both at small and large momenta in a form that is compatible to an acceptable real space interaction potential  $V(\mathbf{r}, \mathbf{r}')$ , as previously investigated in the literature [17].
- [21] The thermodynamic potential is  $\Omega = \Omega_{\text{sp}} + \Omega_{\text{ph}}$ , where the first term is the saddle-point  $\Omega_{\text{sp}} = T S_{\text{sp}}$ , and the second is due to phase fluctuations  $\Omega_{\text{ph}} = \Omega_v + \Omega_c$ . The contribution due to vortices is  $\Omega_v = -T \ln \mathcal{Z}_v$ , where  $\mathcal{Z}_v = \int d\theta_v e^{-S_v}$ . Integration over phase fluctuations  $\theta_c(\mathbf{r}, \tau)$  leads to  $\Omega_c = \Omega_{\text{cm}} + \Omega_{\text{zp}}$ . Here,  $\Omega_{\text{cm}} = \sum_{\mathbf{q}} T \ln [1 - \exp(-\omega_{\mathbf{q}}/T)]$  and  $\Omega_{\text{zp}} = \sum_{\mathbf{q}} \omega_{\mathbf{q}}/2$ , where  $\omega(\mathbf{q}) = c|\mathbf{q}|$  is the frequency and  $c = \sqrt{\rho_s/\kappa_s}$  is the speed of sound.
- [22] D. R. Nelson and J. M. Kosterlitz, Universal jump in the superfluid density of two-dimensional superfluids, *Phys. Rev. Lett.* **39**, 1201 (1977).
- [23] J. M. Kosterlitz, The critical properties of the two-dimensional xy model, *J. Phys. C: Solid State Phys.* **7**, 1046 (1974).
- [24] J. V. José, L. P. Kadanoff, S. Kirkpatrick, and D. R. Nelson, Renormalization, vortices, and symmetry-breaking perturbations in the two-dimensional planar model, *Phys. Rev. B* **16**, 1217 (1977); Erratum: *Phys. Rev. B* **17**, 1477 (1978).
- [25] P. M. Chaikin and T. C. Lubensky, *Principles of condensed matter physics*, Cambridge University Press, 1995.
- [26] R. A. Ferrell and R. E. Glover, Conductivity of superconducting films: A sum rule, *Phys. Rev.* **109**, 1398 (1958).
- [27] M. Tinkham and R. A. Ferrell, Determination of the su-

- perconducting skin depth from the energy gap and sum rule, Phys. Rev. Lett. **2**, 331 (1959).
- [28] M. Tinkham, Introduction to Superconductivity, McGraw-Hill, New York, 1975.
- [29] R. Kubo, Statistical-Mechanical Theory of Irreversible Processes. I. General Theory and Simple Applications to Magnetic and Conduction Problems, J. Phys. Soc. Jpn. **12**, 570 (1957).
- [30] J. P. A. Devreese, J. Tempere and C. A. R. Sá de Melo, Effects of Spin-Orbit Coupling on the Berezinskii-Kosterlitz-Thouless Transition and the Vortex-Antivortex Structure in Two-Dimensional Fermi Gases, Phys. Rev. Lett. **113**, 165304 (2014).
- [31] J. P. A. Devreese, J. Tempere, and C. A. R. Sá de Melo, Quantum phase transitions and Berezinskii-Kosterlitz-Thouless temperature in a two-dimensional spin-orbit-coupled Fermi gas, Phys. Rev. A **92**, 043618 (2015).
- [32] Since the momentum distribution  $n_{sp}(\mathbf{k}) \geq 0$  for any  $\mathbf{k}$ , the result is easily obtained through the successive bounds  $\rho_{s_1} = (ta^2/L^2) \sum_{\mathbf{k}} \cos(k_x a) n_{sp}(\mathbf{k}) \leq (ta^2/L^2) \sum_{\mathbf{k}} |\cos(k_x a)| n_{sp}(\mathbf{k}) \leq (ta^2/L^2) \sum_{\mathbf{k}} n_{sp}(\mathbf{k}) \leq (ta^2/L^2)(N/2) = t\nu/2$ , where we used  $L^2 = N_{si}a^2$  and the filling factor  $\nu = N/N_{si}$ , with  $N_{si}$  being the number of sites and  $N$  being the number of particles.
- [33] J. E. Hirsch and F. Marsiglio, Optical sum rule violation, superfluid weight, and condensation energy in the cuprates, Phys. Rev. B, **62**, 15131 (2000).
- [34] S. Maiti and A. V. Chubukov, Optical integral and sum-rule violation in high- $T_c$  superconductors, Phys. Rev. B **81**, 245111 (2010).
- [35] To represent the interaction  $V_s$  with momentum space range  $k_R$ , we use the use two-body bound state relation  $1/V_s = \sum_{\mathbf{k}} |\Gamma_s(\mathbf{k})|^2 / [2\varepsilon_{\mathbf{k}} - E_B]$ .
- [36] For the conventional s-wave case, the choice of  $V_s/t = 3$  corresponds to onsite interaction  $U/t = -3$  and nearest neighbor interaction  $V/t = 0$  (attractive- $U$  Hubbard model), while for the extended s-wave case, the same choice corresponds to  $U/t = 0$  and  $V/t = -3$  (extended Hubbard model).
- [37] T. Paiva, R. R. dos Santos, R. T. Scalettar, and P. J. H. Denteneer, Critical temperature for the two-dimensional attractive Hubbard model, Phys. Rev. B **69**, 184501 (2004).
- [38] Contributions beyond phase fluctuations arise in the Bose limit (low densities) and lead to logarithmic corrections to  $T_c^0$  due to residual boson-boson interactions. See, e.g., D. S. Fisher, and P. C. Hohenberg, Dilute Bose gas in two dimensions, Phys. Rev. B **37**, 4936 (1988).